

# Longitudinal NSCLC Treatment Progression via Multimodal Generative Models

Massimiliano Mantegna<sup>\*†</sup>, Elena Mulero Ayllón<sup>\*</sup>, Alice Natalina Caragliano<sup>\*</sup>, Francesco Di Feola<sup>‡</sup>  
Claudia Tacconi<sup>§</sup>, Michele Fiore<sup>§¶</sup>, Edy Ippolito<sup>§¶</sup>, Carlo Greco<sup>§¶</sup>, Sara Ramella<sup>§¶</sup>  
Philippe C. Cattin<sup>||</sup>, Paolo Soda<sup>\*††</sup>, Matteo Tortora<sup>\*\*††</sup>, Valerio Guarrasi<sup>\*††</sup>

<sup>\*</sup> Unit of Artificial Intelligence and Computer Systems, Department of Engineering, Università Campus Bio-Medico di Roma, Italy

<sup>†</sup> Multi-Specialist Clinical Institute for Orthopaedic Trauma Care (COT), Messina, Italy

<sup>‡</sup> Department of Diagnostics and Intervention, Radiation Physics, Biomedical Engineering, Umeå University, Sweden

<sup>§</sup> Operative Research Unit of Radiation Oncology, Fondazione Policlinico Universitario Campus Bio-Medico, Rome, Italy

<sup>¶</sup> Research Unit of Radiation Oncology, Department of Medicine and Surgery, Università Campus Bio-Medico di Roma, Italy

<sup>||</sup> Department of Biomedical Engineering, University of Basel, Allschwil, Switzerland

<sup>\*\*</sup> Department of Naval, Electrical, Electronics and Telecommunications Engineering, University of Genoa, Italy

<sup>††</sup> These authors jointly supervised this work and share the last authorship.

**Abstract**—Predicting tumor evolution during radiotherapy is a clinically critical challenge, particularly when longitudinal changes are driven by both anatomy and treatment. In this work, we introduce a *Virtual Treatment (VT)* framework that formulates non-small cell lung cancer (NSCLC) progression as a *dose-aware multimodal conditional image-to-image translation* problem. Given a CT scan, baseline clinical variables, and a specified radiation dose increment, VT aims to synthesize plausible follow-up CT images reflecting treatment-induced anatomical changes. We evaluate the proposed framework on a longitudinal dataset of 222 stage III NSCLC patients, comprising 895 CT scans acquired during radiotherapy under irregular clinical schedules. The generative process is conditioned on delivered dose increments together with demographic and tumor-related clinical variables. Representative GAN-based and diffusion-based models are benchmarked across 2D and 2.5D configurations. Quantitative and qualitative results indicate that diffusion-based models benefit more consistently from multimodal, dose-aware conditioning and produce more stable and anatomically plausible tumor evolution trajectories than GAN-based baselines, supporting the potential of VT as a tool for in-silico treatment monitoring and adaptive radiotherapy research in NSCLC.

**Index Terms**—Medical Imaging, Multimodal, Generative AI, GANs, Diffusion Models, NSCLC, Oncology, Radiotherapy

## I. INTRODUCTION

The increasing integration of artificial intelligence (AI) into clinical workflows is enabling a paradigm shift toward predictive and personalized medicine, particularly in oncology, where decision-making relies on the joint interpretation of imaging, clinical, and treatment-related data [1]–[7]. In this context, *multimodal* learning has emerged as a key strategy for capturing patient-specific disease dynamics, especially in longitudinal scenarios where anatomical changes are driven not only by natural disease progression but also by therapeutic interventions [8]–[12]. Radiotherapy represents a paradigmatic example of such a setting. During treatment, patients routinely

undergo baseline simulation CT for planning, followed by one or more follow-up CT scans acquired at irregular intervals to monitor anatomical changes and treatment response. However, longitudinal imaging in radiotherapy is inherently retrospective: anatomical modifications are observed only after dose delivery, and acquisition schedules vary widely across patients due to toxicity, adaptive re-planning, and logistical constraints [13]. These limitations hinder the ability to anticipate treatment-induced changes and to explore alternative dose-response scenarios.

This challenge is particularly pronounced in non-small cell lung cancer (NSCLC), which accounts for approximately 85% of lung cancer cases and remains the leading cause of cancer-related mortality worldwide [14]. Longitudinal modeling in thoracic CT is further complicated by respiratory motion, variable lung inflation, and complex non-linear deformations involving both tumor and surrounding parenchyma [15]. Despite these difficulties, the delivered radiation dose represents a measurable, controllable, and clinically meaningful driver of anatomical evolution, yet it is rarely incorporated explicitly as a conditioning variable in generative models.

Recent advances in generative AI have demonstrated the potential to synthesize medical images with high fidelity, using Generative Adversarial Networks (GANs) [16]–[18]. While GAN-based image-to-image translation has been widely applied to medical imaging, most methods target static appearance changes or modality conversion and do not explicitly model longitudinal, treatment-driven anatomical evolution [19]. More recently, Diffusion Models (DMs) [20] have shown promising results in modeling spatiotemporal progression by conditioning generation on temporal gaps and clinical variables [21]. However, existing approaches remain confined to neuroimaging, focus on natural aging rather than therapeutic effects, and do not exploit controllable treatment variables such as delivered dose [22].

Corresponding author: Valerio Guarrasi (valerio.guarrasi@unicampus.it)

In this work, we introduce a *Virtual Treatment* (VT) framework that formulates longitudinal NSCLC tumor evolution as a *dose-aware multimodal conditional image-to-image translation* problem. Given a CT scan, patient-specific clinical variables, and a radiation dose increment, VT aims to synthesize plausible follow-up CT scans that reflect treatment-induced anatomical changes. The main contributions of this work are as follows:

- We introduce the first *Virtual Treatment* framework for radiotherapy that explicitly formulates NSCLC evolution prediction as a *dose-aware multimodal conditional image-to-image translation* problem.
- We propose a tumor-focused loss that restricts the reconstruction objective to the Clinical Target Volume (CTV), using the baseline planning segmentation as an anatomical supervision that guides the models toward clinically relevant regions.
- We conduct a benchmarking study comparing GAN-based and diffusion-based generative models across 2D and 2.5D formulations, analyzing their volumetric tumor evolution and computational efficiency under dose-aware multimodal conditioning.

The remainder of the paper is organized as follows: [Section II](#) describes the clinical dataset and acquisition protocol; [Section III](#) presents the VT formulation, including training and inference strategies, and loss design; [Section IV](#) details the model architectures and implementation settings; [Section V](#) reports quantitative and qualitative results; finally, [Section VI](#) summarizes the findings and discusses future directions.

## II. MATERIALS

This study uses a private longitudinal dataset of 222 patients with stage III NSCLC [23] treated with radiotherapy at Fondazione Policlinico Universitario Campus Bio-Medico di Roma. The cohort includes 895 thoracic CT scans, with one baseline simulation CT per patient and multiple follow-up CT scans acquired during treatment. Radiotherapy followed standard protocols with daily fractions of 1.8 Gy or 2.0 Gy, for a prescribed total dose of 60 Gy. Due to adaptive re-planning and protocol variations, the cumulative delivered dose reaches up to 68.4 Gy. Follow-up CT scans were acquired at irregular time points, reflecting real-world clinical practice. On average, each patient underwent  $2.38 \pm 1.31$  follow-up scans.

For each acquisition, the cumulative delivered dose was recorded and used as the only longitudinal clinical variable. Baseline variables collected at treatment planning include age, sex, histological diagnosis, and clinical tumor and nodal staging (cT, cN). A CTV segmentation was available only for the baseline CT, as routinely performed in radiotherapy planning.

### A. Preprocessing

All follow-up CT scans were registered to the corresponding baseline simulation CT using an affine and B-spline transformation. CT intensities were converted to Hounsfield Units, clipped to  $[-900, 300]$  HU [24], and normalized to

$[0, 1]$ . Volumes were resampled to a uniform voxel spacing of  $1 \times 1 \times 3$  mm<sup>3</sup>. Spatial cropping was performed using a fixed in-plane bounding box derived from the largest baseline CTV in the cohort. Along the axial direction, we retained only slices containing the baseline CTV.

Clinical variables were standardized before training. Age and dose values were min–max normalized, sex was encoded as a binary variable, histological diagnosis was one-hot encoded, and cT and cN were encoded as ordinal variables.

The resulting modalities provide consistent, anatomically focused inputs for training the generative models described in [Section III](#).

## III. METHODS

An overview of the proposed multimodal VT framework is shown in [Figure 1](#). *Panel (A)* summarizes the problem setting, and *Panel (B)* outlines the training and inference procedures.

### A. Problem Setting

We formalize the VT as a dose-aware multimodal conditional image-to-image translation task on longitudinal CT scans acquired during radiotherapy. Let  $p \in \{1, \dots, P\}$  denote a patient observed at an irregular sequence of acquisition times:

$$\mathcal{T}_p = \{t_p^{(0)} < t_p^{(1)} < \dots < t_p^{(n_p)}\},$$

where  $t_p^{(j)}$  is the acquisition time of the  $j$ -th CT scan,  $t_p^{(0)}$  is the *baseline* time point, and  $n_p+1$  is the number of scans for patient  $p$ . For simplicity, from this point onward we omit the patient index and write  $t$  in place of  $t_p$ .

At  $t^{(0)}$ , a vector of baseline clinical features  $\mathbf{c}_p \in \mathbb{R}^d$  is collected, where  $d$  is the number of variables (age, sex, tumor diagnosis, cT, cN). These features are reused as conditioning information for all acquisitions in  $\mathcal{T}_p$ . At each  $t \in \mathcal{T}_p$ , a CT volume  $\mathbf{x}_{p,t} \in \mathcal{X} \subset \mathbb{R}^{H \times W \times D}$  is available, where  $H$  and  $W$  denote the in-plane dimensions and  $D$  denote the number of axial slices.

For any ordered pair  $(t, s)$  with  $t < s$  and  $t, s \in \mathcal{T}_p$ , we define the *dose increment*

$$\delta_{p,t \rightarrow s} = d_{p,s} - d_{p,t},$$

which is the additional physical dose (Gy) delivered between two acquisitions.

### B. Virtual Treatment as a generative formulation

Given a current observation  $(\mathbf{x}_{p,t}, \mathbf{c}_p)$  and a dose increment  $\delta_{p,t \rightarrow s}$ , the goal of VT is to learn the conditional distribution

$$p_{\theta}(\mathbf{x}_{p,s} \mid \mathbf{x}_{p,t}, \mathbf{c}_p, \delta_{p,t \rightarrow s}), \quad (1)$$

parameterized by  $\theta$ , which denotes the learnable parameters of the chosen generative model. We model this distribution with an image-to-image generator  $G_{\theta}$  producing a prediction  $\hat{\mathbf{x}}_{p,s}$  of the future scan  $\mathbf{x}_{p,s}$ . Formally:

$$\hat{\mathbf{x}}_{p,s} = G_{\theta}(\mathbf{x}_{p,t}; \mathbf{c}_p, \delta_{p,t \rightarrow s}), \quad (2)$$

*Training.* From the training patients  $\mathcal{P}_{\text{train}}$ , we build a supervised dataset by enumerating *all* ordered scan pairs. For

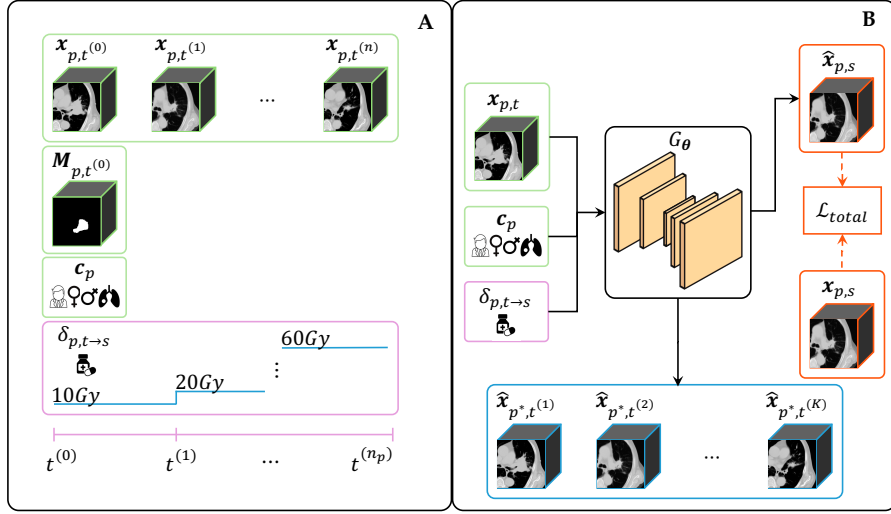


Figure 1: Overview of the proposed multimodal VT framework. **(A) Problem setting.** Multimodal conditioning for virtual treatment forecasting (*green*: input CT and baseline clinical variables; *pink*: dose increment). **(B) Generative formulation.** The generator  $G_\theta$  synthesizes follow-up CTs conditioned on input CT, clinical features, and dose increment, optimized with a reconstruction loss and a tumor-focused term within the CTV (*orange*). Inference follows the *direct dose-response* strategy (*blue*) explained in Section III.

each patient  $p \in \mathcal{P}_{\text{train}}$ , and for every future time point  $s \in \mathcal{T}_p$ , we consider all earlier scans  $t \in \mathcal{T}_p$  such that  $t < s$ , forming a training tuple

$$z = (\mathbf{x}_{p,t}, \mathbf{c}_p, \delta_{p,t \rightarrow s}, \mathbf{x}_{p,s}).$$

The resulting training set is therefore defined as

$$\mathcal{D}_{\text{train}} = \{z : p \in \mathcal{P}_{\text{train}}, t, s \in \mathcal{T}_p, t < s\}. \quad (3)$$

This construction ensures that, for each patient, the model is trained on the complete set of admissible longitudinal transitions: by fixing a target scan  $s$  and collecting all compatible predecessors  $t < s$ , the dataset spans every clinically observed evolution trajectory. As a consequence, each mini-batch contains a heterogeneous mixture of temporal separations ( $s - t$ ) and corresponding dose increments  $\delta_{p,t \rightarrow s}$ , naturally exposing the model to a broad spectrum of progression patterns.

We define the *multimodal conditioning vector*

$$\mathbf{h}_\delta = (\mathbf{c}_p, \delta_{p,t \rightarrow s}),$$

which concatenates baseline clinical variables and dose increment. We use  $\mathbf{h}_\delta$  in Section IV to specify model conditioning.

*Loss function.* We employ a composite loss function  $\mathcal{L}_{\text{total}}$  that combines the standard objective of the generative model with a tumor-focused term:

$$\mathcal{L}_{\text{total}} = \mathcal{L}_{\text{main}} + \lambda \mathcal{L}_{\text{tumor}}, \quad (4)$$

where  $\mathcal{L}_{\text{main}}$  denotes the training objective of the chosen architecture (GAN- or diffusion-based),  $\mathcal{L}_{\text{tumor}}$  encourages accurate reconstruction of the clinically most relevant region, and  $\lambda$  is a hyperparameter controlling the relative weight of the tumor-focused regularization.

The main loss is averaged over all positions  $i \in N$ , where  $N$  corresponds to the set of voxels in image space (GANs) or latent units in the noise prediction space (DMs):

$$\mathcal{L}_{\text{main}}^{\text{GANs}} = \frac{1}{|N|} \sum_{i \in N} \left| \hat{\mathbf{x}}_{p,s}^{(i)} - \mathbf{x}_{p,s}^{(i)} \right|, \quad (5)$$

$$\mathcal{L}_{\text{main}}^{\text{DMs}} = \frac{1}{|N|} \sum_{i \in N} \left| \hat{\epsilon}_{p,s}^{(i)} - \epsilon_{p,s}^{(i)} \right|, \quad (6)$$

where  $\epsilon_{p,s}$  and  $\hat{\epsilon}_{p,s}$  denote the true and predicted noise in the diffusion process, respectively.

To guide learning toward anatomically meaningful changes, we introduce a tumor-focused  $\ell_1$  loss restricted to the CTV of the target scan. Let the tumor mask for patient  $p$  at time  $t$  be denoted by

$$\mathbf{M}_{p,t} \in \{0, 1\}^{H \times W \times D},$$

where  $\mathbf{M}_{p,t}^{(i)} = 1$  if voxel  $i$  belongs to the CTV and 0 otherwise. The number of voxels within the tumor region is

$$|V_{\text{CTV}}| = \sum_i \mathbf{M}_{p,t}^{(i)}.$$

Given a target image  $\mathbf{x}_{p,s}$  and its prediction  $\hat{\mathbf{x}}_{p,s}$ , the tumor loss is defined as

$$\mathcal{L}_{\text{tumor}} = \frac{1}{|V_{\text{CTV}}|} \sum_i \left| \hat{\mathbf{x}}_{p,s}^{(i)} - \mathbf{x}_{p,s}^{(i)} \right| \mathbf{M}_{p,t}^{(i)}, \quad (7)$$

In this work, due to the limited availability of longitudinal tumor segmentations, we rely on a single tumor mask  $\mathbf{M}_{p,t^{(0)}}$  obtained from the baseline planning CT and reused it across all subsequent time points of patient  $p$ . This choice is consistent with clinical practice, where the CTV is routinely delineated

only on the simulation CT for treatment planning and not re-contoured on intermediate follow-up scans.

*Inference.* For an unseen patient  $p^* \in \mathcal{P}_{\text{test}}$ , we adopt a *direct dose-response* strategy: starting from the baseline image  $\mathbf{x}_{p^*,t^{(0)}}$ , we specify a sequence of *dose increments*

$$\delta_{p^*} = \{\delta_{p^*,k}\}_{k=1}^K,$$

each measured with respect to the baseline  $t^{(0)}$ . For each  $\delta_{p^*,k}$  value, the generator produces a dose-conditioned prediction

$$\hat{\mathbf{x}}_{p^*}^{(k)} = G_{\theta}(\mathbf{x}_{p^*,t^{(0)}}; \mathbf{c}_{p^*}, \delta_{p^*,k}).$$

Here,  $K$  denotes the number of dose queries selected by the user, which does not necessarily correspond to the number of clinically acquired follow-up scans. The model can be queried at arbitrary dose levels, including hypothetical values, thus generating a synthetic dose-indexed progression trajectory decoupled from the clinical acquisition schedule.

#### IV. EXPERIMENTAL SETUP

We evaluate the VT framework introduced in Section III by comparing representative GAN-based and diffusion-based models within a unified dose-aware multimodal conditional image-to-image translation setting. All models take as input a CT volume  $\mathbf{x}_{p,t}$  and the conditioning vector  $\mathbf{h}_{\delta}$  defined in Section III and are trained to predict the future scan  $\hat{\mathbf{x}}_{p,s}$  according to Eq. (2). We benchmark two model families: (i) 2D GAN-based architectures (Pix2Pix and CycleGAN) and (ii) a 2.5D diffusion-based model (TADM), which represents state-of-the-art longitudinal forecasting under multimodal conditioning.

##### A. Implementation and Training Details

Experiments use a patient-level hold-out split with 80% of patients for training, 5% for validation, and 15% for testing. Following Eq. (3), we include all ordered scan pairs  $(t, s)$  with  $t < s$ , yielding 78,502 slice-wise paired samples. We also include identity pairs  $(t = s)$  to stabilize near-zero dose predictions.

##### B. 2D GAN-Based Models

We evaluate two representative 2D GAN-based image-to-image translation models, Pix2Pix and CycleGAN, as baselines for dose-conditioned CT synthesis. Both use a ResNet generator with an encoder-bottleneck-decoder structure and PatchGAN discriminators. Pix2Pix is trained in a supervised setting with paired longitudinal CT slices. CycleGAN uses two generators and a cycle-consistency loss to support unpaired translation. In both cases, the conditioning vector  $\mathbf{h}_{\delta}$  is encoded by a shared multi-layer perceptron and injected into the generator bottleneck as a channel-wise modulation, enabling patient- and dose-specific control. Discriminators are kept unconditional to preserve an appearance-driven adversarial objective. Both GANs are trained with an adversarial loss, an  $\ell_1$  reconstruction term, and the proposed tumor-focused loss (Eq. (7)).

##### C. 2.5D Diffusion-Based Model

We adopt TADM [22] as a diffusion-based baseline and adapt it to model treatment-driven, rather than age-driven, anatomical progression.

TADM operates in a 2.5D setting by processing triplets of consecutive axial CT slices. An encoder extracts anatomical context from the input triplet and injects it into a diffusion UNet for conditional denoising. Given an input scan  $\mathbf{x}_{p,t}$ , the model predicts a residual  $\hat{\mathbf{r}}_{p,t \rightarrow s}$  and reconstructs the target scan as:

$$\hat{\mathbf{x}}_{p,s} = \mathbf{x}_{p,t} + \hat{\mathbf{r}}_{p,t \rightarrow s}.$$

Conditioning is implemented by embedding the dose increment  $\delta_{p,t \rightarrow s}$  and the baseline clinical variables  $\mathbf{c}_p$  through separate projection layers. The resulting embeddings modulate the UNet feature maps via additive feature-wise conditioning in each residual block, so that treatment-related and patient-specific information influence denoising throughout the network. TADM is trained with the standard diffusion noise-prediction objective, combined with the tumor-focused loss (Eq. (7)) applied after residual reconstruction.

#### V. RESULTS

In this section, we report the results of our multimodal VT framework for forecasting tumor evolution. All models were evaluated using tumor-specific volumetric error, computational efficiency indicators, and qualitative visual assessment.

All evaluation metrics were computed within a patient-specific *Local* region, defined by the CTV bounding box. This region is clinically the most relevant for assessing treatment response, as it directly captures dose-driven tumor evolution while excluding confounding anatomical variations in surrounding tissues, making it particularly appropriate for evaluating generative forecasting performance.

##### A. Tumor Segmentation Evaluation

To assess whether the models capture treatment-related tumor evolution, we perform a tumor-focused volumetric analysis. Since manual CTV annotations are available only at baseline, tumor extent at follow-up time points is estimated using an Otsu-based thresholding strategy applied to both real and generated CT scans. For each follow-up scan, an Otsu-derived binary mask is extracted and tumor volume is computed as the number of voxels within the thresholded region. The relative volumetric discrepancy between predicted and real tumor volumes is defined as:

$$|\Delta V| = 100 \cdot \frac{|V_{\text{pred}} - V_{\text{real}}|}{V_{\text{real}}},$$

where  $V_{\text{pred}}$  denotes the tumor volume obtained from the Otsu mask of the generated scan, and  $V_{\text{real}}$  denotes the corresponding volume extracted from the real follow-up scan. This metric quantifies the relative deviation of the predicted tumor burden from the reference real volume.

The resulting percentage volumetric discrepancy trends, evaluated as a function of the cumulative dose increment, are reported in Figure 2.

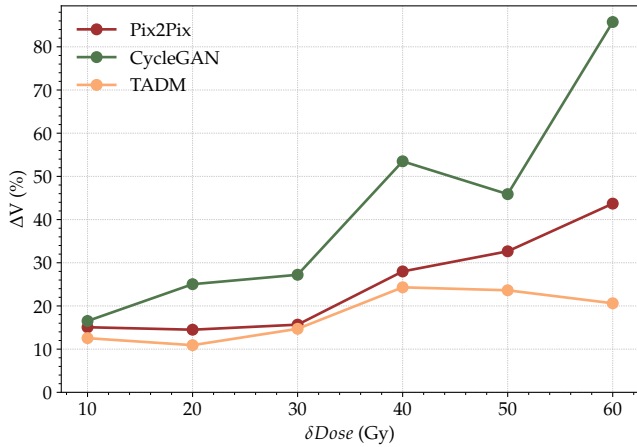


Figure 2: Percentage volumetric discrepancy  $|\Delta V|$  between real and generated segmentations as a function of the dose increment ( $\delta Dose$  (Gy)), aggregated into discrete dose bins (10–60 Gy). Each curve represents one generative model.

As shown by these trends, TADM produces more stable trajectories and moderate variation at higher dose levels. In contrast, CycleGAN and Pix2Pix show the opposite behaviour, with a progressive overestimation of tumor shrinkage that becomes more pronounced for large dose increments. The largest deviations are observed for CycleGAN, which exceeds 80% error at 60 Gy.

Volumetric differences ( $|\Delta V|$ ) within 25% are considered clinically acceptable and are consistent with reported CTV variability in NSCLC radiotherapy (typically 7–25%) [25].

Two conclusions emerge from this analysis: (i) diffusion-based models preserve volumetric dynamics significantly better than GAN-based models and remain closer to real tumor evolution; (ii) all models show reduced accuracy for large dose differences, which confirms the difficulty of forecasting tumor progression over long temporal intervals.

### B. Computational Cost Analysis

Figure 3 relates tumor volume error to computational cost, measured in Giga Multiply-Add Operations per second (GMACs) and number of parameters. A clear accuracy-complexity trade-off emerges: Pix2Pix and CycleGAN are lightweight but show higher volume errors, whereas the diffusion-based TADM achieves substantially improved accuracy at moderate computational cost. Notably, the gap between training and inference cost differs markedly across models. When transitioning from training to inference, the number of required operations is reduced by approximately 53% for CycleGAN, 8% for Pix2Pix, and 78% for TADM, highlighting a substantially more favorable deployment profile for diffusion-based forecasting in longitudinal settings. These results indicate that model evaluation for radiotherapy forecasting should jointly consider predictive accuracy and computational efficiency, particularly in longitudinal settings requiring large-scale virtual inference.

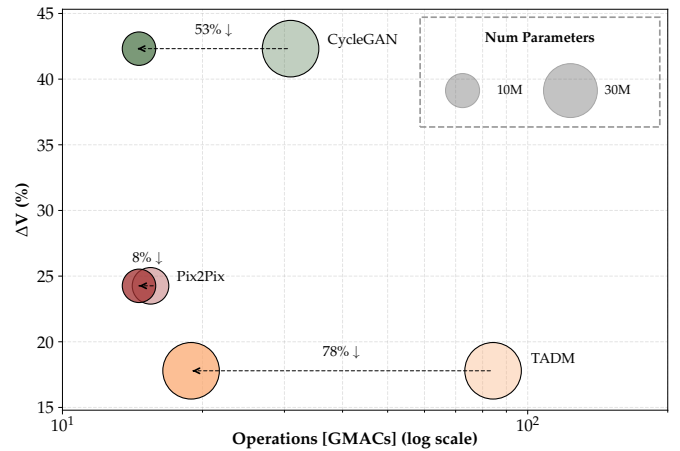


Figure 3: Comparison of models in terms of  $|\Delta V|$  error (y-axis) and computational cost measured in GMACs (x-axis, log scale) for the training (*darker bubbles*) and inference (*lighter bubbles*) phases. Bubble size is proportional to the number of model parameters (10M and 30M).

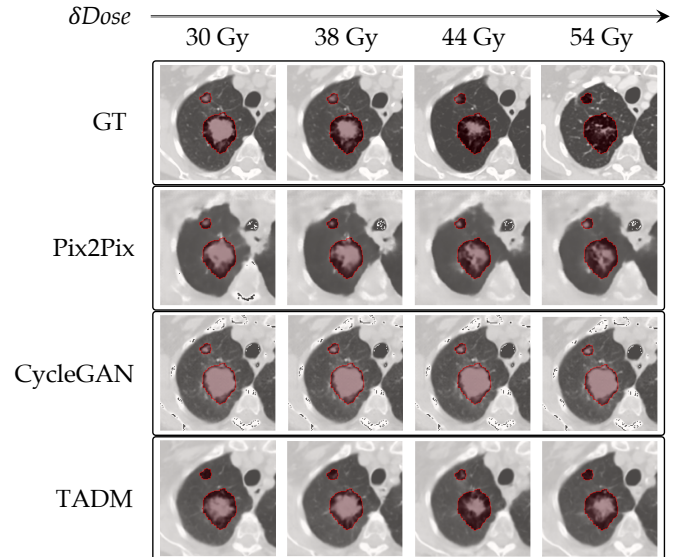


Figure 4: Qualitative comparison across increasing dose levels for a representative patient treated with a 2 Gy/day fractionation protocol. Columns correspond to increasing cumulative dose, while rows show the GT follow-up CT and the predictions generated by each model. The red contour indicates the CTV region used for *Local* analysis.

### C. Qualitative Results

Figure 4 shows representative qualitative results for a patient treated with a 2 Gy/day fractionation scheme, illustrating model behavior across increasing dose levels. Predictions from each model are shown alongside the ground truth (GT), enabling a longitudinal visual assessment of tumor evolution within the CTV region. Consistent with quantitative findings, GAN-based models (Pix2Pix and CycleGAN) show limited

ability to capture dose-driven tumor regression. Pix2Pix tends to preserve tumor appearance across dose levels, resulting in nearly static trajectories and overestimation of residual tumor volume. CycleGAN further introduces high-frequency artifacts and unstable local deformations, leading to inconsistent volumetric trends. In contrast, the diffusion-based TADM model captures a progressive, dose-dependent reduction of tumor extent that closely follows the trend observed in real follow-up CTs, indicating improved modeling of treatment-induced anatomical change. At high cumulative doses, diffusion-based predictions may overestimate tumor regression, occasionally producing overly aggressive shrinkage. This behavior reflects uncertainty in late-stage tumor morphology and highlights the intrinsic difficulty of long-range longitudinal forecasting.

## VI. CONCLUSIONS

We presented a multimodal VT framework for forecasting longitudinal CT evolution in NSCLC patients undergoing radiotherapy, comparing 2D GAN-based and 2.5D diffusion-based models under explicit dose-aware conditioning. To the best of our knowledge, this is the first study to systematically investigate treatment-driven anatomical forecasting in thoracic CT with multimodal generative models. Longitudinal tumor prediction proved inherently challenging due to irregular acquisition schedules, non-uniform tumor regression, and the lack of longitudinal annotations. Despite these limitations, diffusion-based models demonstrated greater robustness and produced more stable volumetric predictions across dose increments, whereas GAN-based models exhibited progressive error accumulation and overestimation of tumor shrinkage at higher doses. From a practical perspective, diffusion-based modeling achieved a more favorable accuracy-efficiency trade-off, with TADM providing the best balance between predictive stability and computational cost. Future work will focus on integrating richer clinical descriptors, extending the framework to fully 3D diffusion models, and incorporating physics-informed priors and longitudinal segmentations [26], [27] to further constrain long-range tumor evolution. Overall, the proposed VT framework represents a promising step toward in-silico treatment monitoring and adaptive radiotherapy support in NSCLC.

## ACKNOWLEDGMENTS

Massimiliano Mantegna and Alice Natalina Caragliano are PhD students enrolled in the National PhD program in Artificial Intelligence, in the XXXVIII and XXXIX cycle, respectively, course on Health and life sciences, organized by Università Campus Bio-Medico di Roma. We also acknowledge partial financial support from: i) Università Campus Bio-Medico di Roma within the project “AI-powered Digital Twin for next-generation lung cancer care (IDEA)”, ii) JCSMK24-0094, iii) Cancerforskningsfonden Norrland project LP 25-2383. Resources are provided by NAISS and SNIC at Alvis @ C3SE (grants no. 2022-06725 and 2018-05973).

## REFERENCES

[1] N. J. Schork, *Artificial intelligence and personalized medicine*, in: *Precision medicine in Cancer therapy*, Springer, 2019, pp. 265–283.

[2] M. Tortora, et al., RadioPathomics: multimodal learning in non-small cell lung cancer for adaptive radiotherapy, *IEEE Access* 11 (2023) 47563–47578.

[3] C. M. Caruso, et al., A deep learning approach for overall survival prediction in lung cancer with missing values, *Computer Methods and Programs in Biomedicine* 254 (2024) 108308.

[4] D. Paolo, et al., Predicting lung cancer survival with attention-based CT slices combination, *Health Information Science and Systems* 14 (1) (2026) 20.

[5] L. Nibid, et al., Deep pathomics: A new image-based tool for predicting response to treatment in stage iii non-small cell lung cancer, *Plos one* 18 (11) (2023) e0294259.

[6] A. N. Caragliano, et al., Doctor-in-the-loop: An explainable, multi-view deep learning framework for predicting pathological response in non-small cell lung cancer, *Image and Vision Computing* 161 (2025) 105630.

[7] C. Z. Liu, et al., Exploring deep pathomics in lung cancer, in: *2021 IEEE 34th International Symposium on Computer-Based Medical Systems (CBMS)*, IEEE, 2021, pp. 407–412.

[8] A. N. Caragliano, et al., Multimodal doctor-in-the-loop: A clinically-guided explainable framework for predicting pathological response in non-small cell lung cancer, in: *2025 International Joint Conference on Neural Networks (IJCNN)*, 2025, pp. 1–8.

[9] V. Guarrasi, et al., A systematic review of intermediate fusion in multimodal deep learning for biomedical applications, *Image and Vision Computing* (2025) 105509.

[10] M. Baumann, et al., Radiation oncology in the era of precision medicine, *Nature Reviews Cancer* 16 (4) (2016) 234–249.

[11] C. M. Caruso, et al., MARIA: A multimodal transformer model for incomplete healthcare data, *Computers in Biology and Medicine* 196 (2025) 110843.

[12] E. Cordelli, et al., Machine learning predicts pulmonary long covid sequelae using clinical data, *BMC Medical Informatics and Decision Making* 24 (1) (2024) 359.

[13] J. Bertholet, et al., Real-time intrafraction motion monitoring in external beam radiotherapy, *Physics in medicine & biology* 64 (15) (2019) 15TR01.

[14] H.-U. Kauczor, et al., ESR/ERS statement paper on lung cancer screening, *European radiology* 30 (2020) 3277–3294.

[15] H. Xiao, et al., Deep learning-based lung image registration: A review, *Computers in biology and medicine* 165 (2023) 107434.

[16] L. Tronchin, et al., Beyond a single mode: GAN ensembles for diverse medical data generation, *Computer Methods and Programs in Biomedicine* 277 (2026) 109234.

[17] M. Mantegna, et al., Benchmarking GAN-Based vs Classical Data Augmentation on Biomedical Images, in: *International Conference on Pattern Recognition*, Springer, 2024, pp. 92–104.

[18] V. Guarrasi, et al., Whole-Body Image-to-Image Translation for a Virtual Scanner in a Healthcare Digital Twin, in: *2025 IEEE 38th International Symposium on Computer-Based Medical Systems (CBMS)*, IEEE, 2025, pp. 528–534.

[19] M. Loni, et al., A review on generative AI models for synthetic medical text, time series, and longitudinal data, *npj Digital Medicine* 8 (2025).

[20] J. Ho, et al., Denoising diffusion probabilistic models, *Advances in neural information processing systems* 33 (2020) 6840–6851.

[21] K. Zhang, et al., Development-driven diffusion model for longitudinal prediction of fetal brain mri with unpaired data, *IEEE Transactions on Medical Imaging* (2024).

[22] M. Litrico, et al., TADM: Temporally-aware diffusion model for neurodegenerative progression on brain mri, in: *International Conference on Medical Image Computing and Computer-Assisted Intervention*, Springer, 2024, pp. 444–453.

[23] *AJCC Cancer Staging Manual*, Springer, 2017.

[24] J. Joseph, Deep learning driven image-based cancer diagnosis (2025).

[25] N. Vu, et al., Tumor volume shrinkage during stereotactic body radiotherapy is related to better prognoses in patients with stage I non-small-cell lung cancer, *Journal of Radiation Research* 61 (5) (2020) 740–746.

[26] E. M. Ayllón, et al., Can Foundation Models Really Segment Tumors? A Benchmarking Odyssey in Lung CT Imaging, in: *2025 IEEE 38th International Symposium on Computer-Based Medical Systems (CBMS)*, IEEE, 2025, pp. 375–380.

[27] E. M. Ayllón, et al., Context-Gated Cross-Modal Perception with Visual Mamba for PET-CT Lung Tumor Segmentation, *arXiv preprint arXiv:2510.27508* (2025).